American Mineralogist, Volume 64, pages 224–228, 1979

Measurement of the oxygen fugacity of the cobalt–cobalt oxide buffer assemblage

JONATHAN MYERS AND WILLIAM DANIEL GUNTER

Department of Geology, University of Wyoming
Laramie, Wyoming 82071

Abstract

A thermogravimetric balance with a controlled atmosphere furnace and electrochemical oxygen sensor was calibrated with the oxygen buffer assemblages nickel–bunsenite and wüstite–iron and used to measure the equilibrium fO_2 of the cobalt–cobalt oxide pair between 750° and 1300°C at one atmosphere pressure. The data are represented by the equation:

$$\log fO_2\ (\text{atm}) = 7.936 - 25070/°\text{K} \qquad \sigma = 0.02$$

The total uncertainty is estimated to be ± 0.08 log fO_2 units. This oxygen buffer will be useful for hydrothermal experimentation where fO_2 conditions slightly more reducing than those of the fayalite–magnetite–quartz buffer need to be maintained.

Introduction

The successful use of hydrostatic buffering techniques (see Huebner, 1971) at elevated temperatures and pressures partially depends on the availability of a series of oxygen buffers whose temperature–oxygen fugacity relationships are well known. We present data for the cobalt–cobalt oxide buffer. A thermogravimetric technique using a one-atmosphere gas-mixing furnace containing an oxygen-sensitive electrode was employed to determine the stability of the cobalt–cobalt oxide buffer pair as a function of oxygen fugacity and temperature. This technique is similar to that used by Friel *et al.* (1977) to determine armalcolite stability, except that fO_2 was adjusted to maintain a constant weight of the buffer assemblage for the duration of an experiment.

Experimental procedure

A platinum non-inductively wound furnace having a reaction tube 1.6 cm I.D. was mounted vertically on a hydraulic jack. Two Pt–$Pt_{87}Rh_{13}$ thermocouples and a $(ZrO_2)_{85}(CaO)_{15}$ ceramic oxygen sensor were inserted through the bottom of the furnace and positioned in the hot spot. The temperature gradient over the five-centimeter-long hot spot was 0.4°C/cm at 1200°C. One thermocouple was placed inside the sensor and one outside. The thermocouple inside the sensor shared the platinum lead of the sensor. Pure O_2 flowed internally through the sensor ($\simeq 10$ cc/min) and acted as the sensor reference gas. Both temperature and fO_2 were monitored by millivolt meters of the appropriate impedance.

The charge consisted of a 500 mg mixture of a metal and its oxide: iron–wüstite (IW), nickel–bunsenite (NNO), or the cobalt–cobalt oxide (Co–CoO) buffer pair. The iron, nickel and cobalt were all 99.999 purity from SPEX (lot 07751, 03761, and 04761 respectively). The oxides were prepared by oxidation of the metals in the furnace. The charge, contained in an 0.64 cm O.D. alumina crucible, was held in the furnace hot spot by a platinum wire suspended from a Sartorius (type 4406) electronic microbalance. The furnace atmosphere and charge were isolated from the external atmosphere by elevating the furnace to form a cone-in-cone teflon seal with the balance. The charge was reduced or oxidized by varying the composition of a CO_2–H_2 mixture supplied by a gas-mixing train similar to that described by Williams and Mullins (1975), with the exception that in most of our experiments the gas mixing was done in a glass cell containing a magnetic stirring bar, at a flow rate of 100 cc/min.

A Pt–$Pt_{87}Rh_{13}$ thermocouple contained in an alumina sheath (the external thermocouple) and a grounded chromel–alumel thermocouple (the standard thermocouple) sheathed in inconel (Omega part CAIN-116G) were calibrated against the melting points of NaCl (800.6°C) and gold (1064.4°C) by suspending a quartz bucket containing the NaCl or gold in the hot spot of the furnace in a CO_2–H_2 gas

0003–004X/79/0102–0224$02.00

flow of 100 cc/min. The composition of the CO_2–H_2 mixture did not change either thermocouple EMF at the melting point of gold. The external thermocouple was used to monitor the temperature during each experiment and was checked against the standard thermocouple at periodic intervals. However, the temperature recorded inside the oxygen sensor by the internal thermocouple was 6°C lower than that recorded outside by the external thermocouple for CO_2-rich gas mixtures. No horizontal gradients were found across the hot zone of the reaction tube with the sensor in place. The temperature difference did not decrease when the flow of reference gas was halted. It did, however, depend on the furnace gas mixture used; the smallest temperature difference (Δ2°C) was achieved by using pure H_2 as the furnace gas, perhaps reflecting the much greater thermal conductivity of H_2. Conversion of millivolts to fO_2 for an isothermal system can be made from the equation

$$E = \frac{RT}{4F} \ln fO_2(\text{gas mixture}) - \frac{RT}{4F} \ln fO_2(\text{reference}) \qquad (1)$$

where E is the voltage of the oxygen cell in millivolts; fO_2, the oxygen fugacity in atmospheres; T, the temperature in degrees Kelvin; R, the gas constant; and F, the Faraday constant. A non-isothermal system requires the addition of a term to equation (1):

$$E = \frac{RT_e}{4F} \ln fO_2(\text{gas mixture}) - \frac{RT_i}{4F} \ln fO_2(\text{reference}) + \frac{1}{4F}[G^0(O_2, T_e) - G^0(O_2, T_i)] \qquad (2)$$

where T_e is the external temperature, T_i is the temperature measured inside the oxygen probe; and $G^0(O_2)$ is the free energy of O_2 at one atmosphere in calories. Since pure oxygen was used as the reference gas inside the probe,

$$\ln fO_2(\text{reference}) = 0$$

and equation (2) reduces to

$$E = 0.04960 T_e \log fO_2(\text{gas mixture}) + 0.01084[G^0(O_2, T_e) - G^0(O_2, T_i)] \qquad (3)$$

If pure oxygen is used as the furnace gas as well as the reference gas, then equation (3) reduces to

$$E = 0.01084[G^0(O_2, T_e) - G^0(O_2, T_i)] \qquad (4)$$

For an observed difference of 6° between T_e and T_i using oxygen as both the reference and furnaces gases, E was calculated to be −3mV from equation (4). However, the measured E under these conditions was only ±1mV, essentially zero considering experimental errors, and the cell appeared to be responding isothermally. Therefore, we have considered that the difference between T_e and T_i may in part be attributable to real differences between the two thermocouples, and since only the external thermocouple could be calibrated, T_e and equation (1) were used in calculating our results. But the dependence of T_e–T_i on the furnace gas, as noted before, suggests that other not presently understood factors may have been operative. For this reason, the temperature difference was added to the experimental uncertainty.

A basic run consisted of progressively increasing (or decreasing) the furnace temperature in stages while maintaining a null point on the balance (constant weight of the buffer assemblage) by adjusting the gas mixture at each stage. The fO_2 was recorded at the null point at each successive temperature. Any oxidation or reduction (*i.e.* addition or removal of oxygen from the charge) would cause a departure from the null point of the balance. A perturbation of 4 μg, which constituted a reversal, was made on either side of the null point by varying the gas mixture at each temperature. In addition, the null point fO_2 obtained from both heating and cooling cycles did not show any hysteresis. An identical reversed fO_2 value approached from both a higher and lower temperature was our equilibrium criterium.

Uncertainties, expressed in $\log fO_2$ units, are ±0.03 due to the temperature difference measured between the two thermocouples, ±0.01 from the 2° temperature gradient over the furnace hot spot, ±0.01 from a 2° temperature fluctuation which occurred during an isothermal reversal, and ±0.03 which was the magnitude of the $\log fO_2$ shift needed to see a ±4 μg change in weight from the null point. Therefore, total uncertainty is ±0.08 $\log fO_2$ units.

Calibration of system

The uncertainty introduced by the discrepancy between T_i and T_e was further tested by using the NNO and IW buffers as standards. These buffers were chosen because they bracket Co–CoO fO_2 values and because they equilibrate relatively rapidly.

The fayalite–magnetite–quartz (FMQ) buffer was not used, as it involves the transfer of Fe and Si from one phase to another during oxidation or reduction. We found such cation transfer to be extremely sluggish compared to the equilibration times of a few minutes for NNO and Co–CoO and several hours for IW. Exploratory runs with wüstite–magnetite (WM) involved equilibration times of four hours at 1000°C. As the accuracy of the standards used is of concern, we will briefly examine the significance of the varying reaction rates in this respect.

Wüstite in equilibrium with iron has an oxygen-to-iron ratio which varies between 1.05 to 1.06, while wüstite in equilibrium with magnetite varies between 1.09 to 1.18 between 700 and 1300°C (Rizzo *et al.*, 1969, Table 4). We attribute the relative sluggishness of the IW or WM reaction to a non-gaseous reaction. Along an isotherm, the equilibrium composition of wüstite depends on the fO_2, but magnetite or iron can only be in stable equilibrium with wüstite of fixed stoichiometry. On a furnace heating or cooling cycle the wüstite must continuously change composition to remain in equilibrium with the magnetite or iron. In the case of IW the reaction would necessarily be of the form

$$FeO \leftrightarrows Fe_{1-x}O + xFe \qquad (5)$$

A gas phase cannot be involved in this reaction because the bulk composition of the solid assemblage is held constant by maintaining a null point on the balance. The reaction to be calibrated is of the form

$$Fe + \tfrac{1}{2}O_2 \leftrightarrows FeO \qquad (6)$$

If only this reaction occurred the IW buffer would equilibrate rapidly, as no mass transfer is required beyond that to cause the 4 μg balance pertubation. However, to change the stoichiometry of the wüstite by 0.1 percent by reaction (5) would require the transfer of 60 μg of material for an 0.5-gram sample, and hence the apparent sluggishness of reaction (6) and drift of the null point fO_2 sympathetically to the composition of the wüstite. Consequently we think that the phases in the NNO or Co–CoO equilibria maintain their stoichiometry between 700 and 1300°C because of the rapidity of equilibration through heating and cooling cycles.

Temperature–fO_2 data were fitted to a first degree equation on the assumption that ΔH^0 of the reaction is independent of temperature. This assumption is probably valid when the stoichiometry of the solid phases does not change. Uncertainty components are the same that were used by Huebner and Sato (1970) [*i.e.* the standard deviation (σ) and the standard error of the mean], assuming all variation to be in the oxygen fugacity, the dependent variable.

Our data-fit for NNO based on 12 reversals (Table 1) between 800 and 1300°C is

$$\log fO_2\ (\pm 0.01) = 9.346 - 24920/T \qquad \sigma = 0.02$$

The greatest departure of the reversals from the regressed line was 0.03 log units. These data agree extremely well with those given by Huebner and Sato (1970, equation 4′). The predicted log fO_2 values of our equation agree with theirs to within 0.01 log units over the temperature range of their investigation (500–1300°C), and are well within the systematic error of ±0.1 log units which they proposed (see Table 1).

Our measurements also agree to within 0.1 log units of the electrochemical measurements of Charette and Flengas (1968), Tretjakow and Schmalzried (1965), and Taylor and Schmalzried (1964).

Our data-fit for IW based on 9 reversals (Table 1) between 800 and 1300°C is

$$\log fO_2\ (\pm 0.01) = 7.184 - 28040/T \qquad \sigma = 0.03$$

The greatest departure of the reversals from the regressed line is 0.05 log units. Our data agree with those given by Huebner (1975) between 1150 and 1300°C but not with Eugster and Wones' (1962) equation obtained from Darken and Gurry's (1945) data. Our predicted values for log fO_2 differ by as much as 0.16 log units from theirs between 800 and 1300°C. However, there is agreement at 1100°C, the lowest temperature of Darken and Gurry's experiments.

Measurements at lower temperatures made by Tretjakow and Schmalzried (1965), Charette and Flengas (1968) and Rizzo *et al.* (1969) lie at higher fO_2 values than our results. Over the temperature range that their data overlap ours, the discrepancies are less than 0.14 log units and are generally much smaller.

The differences between all these data sets may be due to slight differences in the stoichiometry of wüstite coexisting with iron at the same temperature (see Rizzo *et al.*, 1969, Table 4), or due to an fO_2 gradient between the oxygen probe and the sample because the furnace gases did not equilibrate (see Huebner, 1975). Our balance null-point technique of measuring fO_2 reversals on both heating and cooling cycles, which shows no detectable hysteresis, indicates that our system reached stable equilibrium at 1300°C. Since the oxygen probe and the sample are both within the isothermal region of the furnace, and there is excellent agreement between our NNO data and the published data, we do not think that an fO_2 gradient

Table 1. Experimental results at one atmosphere

Heating Cycle T°C	Probe EMF*	Probe log f_{O_2}	Calc log f_{O_2} this paper	Calc† log f_{O_2}	Cooling Cycle T°C	Probe EMF*	Probe log f_{O_2}	Calc log f_{O_2} this paper	Calc† log f_{O_2}	Buffer
1301	-507	- 6.49	- 6.49	- 6.48	1298	- 506	- 6.49	- 6.52	- 6.51	NNO
1204	-551	- 7.52	- 7.53	- 7.52	1203	- 554	- 7.57	- 7.54	- 7.53	"
1099	-598	- 8.79	- 8.82	- 8.81	1102	- 600	- 8.80	- 8.78	- 8.77	"
1000	-648	-10.26	-10.23	-10.22	999	- 644	-10.21	-10.25	-10.24	"
902	-692	-11.87	-11.86	-11.86	907	- 688	-11.76	-11.77	-11.77	"
799	-738	-13.88	-13.90	-13.90	806	- 737	-13.77	-13.75	-13.74	"
1297	-832	-10.68	-10.68	-10.76	1302	- 827	-10.59	-10.62	-10.71	IW
1192	-870	-11.97	-11.96	-12.01	-	-	-	-	-	"
1188	-874	-12.06	-12.01	-12.06	-	-	-	-	-	"
-	-	-	-	-	1100	- 903	-13.26	-13.24	-13.25	"
-	-	-	-	-	994	- 937	-14.91	-14.95	-14.91	"
-	-	-	-	-	992	- 938	-14.95	-14.98	-14.94	"
-	-	-	-	-	899	- 972	-16.72	-16.74	-16.65	"
-	-	-	-	-	799	-1011	-19.01	-18.97	-18.82	"
1302	-621	- 7.95	- 7.98	- 8.10	1300	- 626	- 8.02	- 8.00	- 8.12	Co–CoO
1201	-662	- 9.05	- 9.07	- 9.17	-	-	-	-	-	"
1196	-664	- 9.11	- 9.13	- 9.22	-	-	-	-	-	"
1097	-706	-10.39	-10.36	-10.42	1100	- 704	-10.34	-10.32	-10.38	"
997	-745	-11.83	-11.80	-11.82	1001	- 742	-11.74	-11.74	-11.76	"
905	-781	-13.37	-13.35	-13.32	902	- 781	-13.40	-13.40	-13.38	"
-	-	-	-	-	852	- 801	-14.35	-14.35	-14.30	"
800	-822	-15.45	-15.43	-15.35	798	- 821	-15.46	-15.47	-15.39	"
765	-834	-16.20	-16.22	-16.12	762	- 835	-16.27	-16.29	-16.18	"

† NNO from Huebner and Sato (1970, equation 4'); IW from Eugster and Wones (1962, table 2); Co–CoO from Chou (in press).

* Recorded EMF is the average between that at which a noticeable weight increase and that at which a noticeable weight decrease was recorded by pertubation from the balance null point.

exists in the isothermal region of the reaction tube. Further experiments should be undertaken to clarify the reasons for these discrepancies. Therefore, we do not recommend extrapolation of fO_2 for the IW buffer. On the other hand, we have shown that for a strictly stoichiometric phase such as bunsenite, we are able to extrapolate safely to 500°C for NNO, and that our cell measurements are in exact agreement with those of Huebner and Sato (1970) for this buffer.

Co–CoO buffer

Fifteen reversals (Table 1) were completed between 750 and 1300°C with Co–CoO. Our data fit the expression

$$\log fO_2\ (\pm 0.01) = 7.936 - 25070/T \qquad \sigma = 0.02$$

The greatest departure of the reversals from the regressed line is 0.03 log units. Our predicted values of log fO_2 agree exactly with the results from the hydrothermal experiments of Chou (1978) at 750 and 700°C. However, at 800 and 600°C his log fO_2 values lie above our curve (Fig. 1) by 0.16 to 0.29 log units. We think the extrapolation of our data from 750 to 600°C for the Co–CoO buffer is warranted, in view of the excellent agreement of our extrapolated data with the measured values of Huebner and Sato (1970) for the NNO equilibrium from 800 to 500°C.

Electrochemical measurements by Tretjakow and Schmalzried (1965) and Taylor and Schmalzried (1964) bracket our data to within 0.1 log units. However, calculations based on free energy data from Robie and Waldbaum (1968) suggest a lower fO_2 at low temperatures and higher fO_2 at high temperatures than that obtained from our study; similar discrepancy was noted in the calculation of fO_2 for NNO and IW buffers from the data of Robie and Waldbaum.

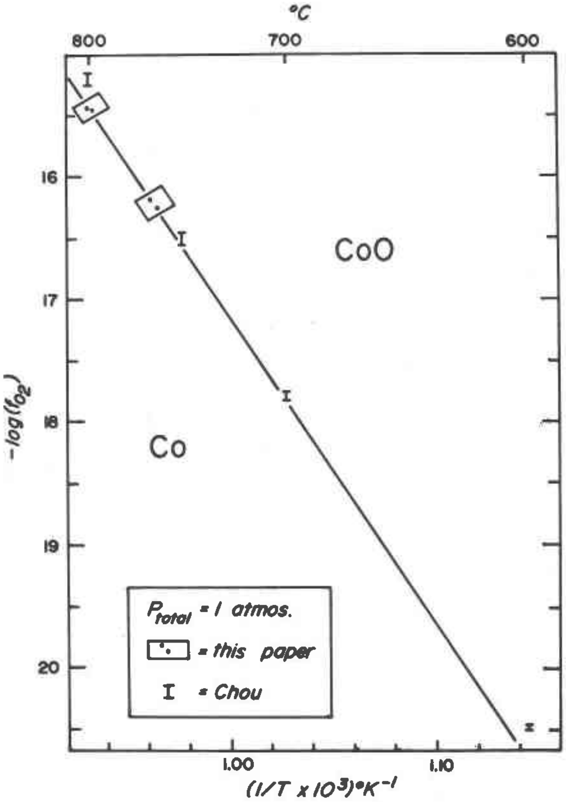

Fig. 1. Experimental data for the Co–CoO buffer at 1 atm total pressure. The straight line is the least-squares fit of our data between 1300 and 750°C. The position of each data symbol represents two reversed experiments, and the length of the data symbol of Chou (1978) corresponds to the maximum spread in the data from his reversals. The position of our reversals is indicated by the two dots inside each rectangle. The width of the $\pm 2\sigma$ envelope about the least-squares fit would be 0.08 log fO_2 units wide. This is too small to illustrate on the scale of the diagram.

Summary and conclusions

The Co–CoO buffer is about an order of magnitude more reducing than the FMQ buffer, being only 0.07 log fO_2 units more reducing at 400°C and 0.64 units more reducing at 1300°C. Hence, it produces geologically significant fO_2 values. The Co–CoO pair should be a useful buffer in hydrothermal experiments because it equilibrates rapidly, it alloys with platinum relatively slowly, and it has a large buffer capacity per unit volume, characteristics it shares with the NNO buffer.

The introduction of a balance into the gas-mixing furnace greatly increases the sensitivity of this technique to oxidation–reduction reactions. The elimination of small errors, such as the ΔT between the furnace and probe, becomes important in further refinements. Using the balance technique, together with calibrations based on standard buffers, we should in the future be able to achieve uncertainties of less than ±0.01 log fO_2 units relative to the standards for experiments performed in a gas-mixing furnace.

Acknowledgments

This work was supported in part by NSF grant DES 75-01293. We acknowledge helpful discussions with Dick Williams, Hans Eugster, and I-Ming Chou during construction of the furnace and subsequent experiments. Thanks are also extended to Dick Williams, George Pajari Jr., Jim Wood, J. S. Huebner, and D. H. Lindsley for their critical reviews of this paper.

References

Charette, G. G. and S. N. Flengas (1968) Thermodynamic properties of the oxides of Fe, Ni, Pb, Cu and Mn by EMF measurements. *J. Electrochem. Soc., 115*, 796–804.

Chou, I-M. (1978) Calibration of oxygen buffers at elevated *P* and *T* using the hydrogen fugacity sensor. *Am. Mineral., 63*, 690–703.

Darken, L. S. and R. W. Gurry (1945) The system iron–oxygen I. The wüstite field and related equilibria. *J. Am. Chem. Soc., 67*, 1398–1412.

Eugster, H. P. and D. R. Wones (1962) Stability relations of the ferruginous biotite, annite. *J. Petrol., 3*, 82–125.

Friel, J. F., R. I. Harker and G. C. Ulmer (1977) Armalcolite stability as a function of pressure and oxygen fugacity. *Geochim. Cosmochim. Acta, 41*, 403–410.

Huebner, J. S. (1975) Oxygen fugacity values of furnace gas mixtures. *Am. Mineral., 60*, 815–823.

——— (1971) Buffering techniques for hydrostatic systems at elevated pressures. In G. C. Ulmer, Ed., *Research Techniques for High Pressure and High Temperature*, p. 123–178. Springer-Verlag, New York.

——— and M. Sato (1970) The oxygen fugacity–temperature relationships of manganese oxide and nickel oxide buffers. *Am. Mineral., 55*, 934–952.

Rizzo, H. F., R. S. Gordon and I. B. Cutler (1969) The determination of phase boundaries and thermodynamic functions in the iron–oxygen system by E.M.F. measurements. *J. Electrochem. Soc., 116*, 266–274.

Robie, R. A. and D. R. Waldbaum (1968) Thermodynamic properties of minerals and related substances at 298.15°K and one atmosphere (1.013 bars) pressure and at higher temperatures. *U.S. Geol. Surv. Bull. 1259.*

Sato, M. (1971) Electrochemical measurements and control of oxygen fugacity and other gaseous fugacities with solid electrolyte sensors. In G. C. Ulmer, Ed., *Research Techniques for High Pressure and High Temperature*, p. 43–99. Springer-Verlag, New York.

Taylor, R. W. and H. Schmalzried (1964) The free energy of formation of some titanites, silicates and magnesian aluminate from measurements made with galvanic cells involving solid electrolytes. *J. Phys. Chem., 68*, 2444–2449.

Tretjakow, V. J. D. and H. Schmalzried (1965) Zur Thermodynamik von Spinellphasen (Chromite, Ferrite, Aluminate). *Ber. Bunsengesellschaft Phys. Chem., 69*, 396–402.

Williams, R. J. and O. Mullins (1976) A system using solid ceramic oxygen electrolyte cells to measure oxygen fugacities in gas mixing systems. *NASA TM X-58167*. National Aeronautics and Space Administration, Lyndon B. Johnson Space Center, Houston.

Manuscript received, January 16, 1978;
accepted for publication, June 15, 1978.